Stopping power of extended cluster and ion charge distributions in an arbitrarily degenerate electron fluid

A. Bret and C. Deutsch
Laboratoire de Physique des Gaz et des Plasmas, Université Paris XI, 91405 Orsay, France
(Received 10 June 1992)

The stopping power of an extended charge distribution at any velocity by a free-electron gas is calculated in the random-phase approximation at any degeneracy. Asymptotic expressions are given in the low- and high-velocity range for any charge distribution with spherical symmetry. We pay attention to the determination of the critical distances of pointlike behavior for an extended charge and uncorrelated behavior for two separated charges. The particular cases of randomly orientated dicluster and atomic ion with extended charges distribution are given particular attention.

PACS number(s): 52.25.Tx, 34.50.Bw, 36.40.+d

I. INTRODUCTION

In close connection with beam-target interaction problems encountered in inertial confinement fusion (ICF) [1,2], it is useful to evaluate the stopping power of projectile ions in a homogeneous and dense electron fluid at any temperature. Considering some pointlike ions, Maynard and Deutsch [3] already completed this task. Recently, clusters of heavy ion beams have been proposed [4] instead of atomic ions. It then appears that correlations within ions in cluster produce a non-negligible influence upon their stopping power. In the degenerate case, a dimensionless quantity quantifying coupling is

$$\chi^2=\frac{1}{\pi q_F a_0}=\frac{V_0}{mV_F}=\frac{1}{\pi}\left[\frac{I_H}{k_B T_F}\right]^{1/2}=\frac{\alpha r_s}{\pi}\ , \qquad (1)$$

with a_F, V_F, and T_F denoting Fermi wave number, velocity, and temperature, respectively. a_0, V_0, and I_H refer to the Bohr radius, velocity, and energy. $r_s=(\frac{4}{3}\pi N_e)^{-1/3}a_0^{-1}$ in terms of the free-electron density N_e, while $\alpha=(9\pi/4)^{-1/3}$. At high temperature ($T\gg T_F$) the random-phase approximation (RPA) is valid when the kinetic energy of the gas is much larger than its potential energy, thus we have ($T_e=T/T_F$)

$$\Gamma_e=\frac{3\pi\chi^2}{2T_e}=\frac{e^2}{k_B T R_{ee}}\ll 1\ , \qquad (2)$$

in terms of $R_{ee}=(\frac{4}{3}\pi N_e)^{-1/3}$ and of the classical plasma parameter Γ_e. At any degeneracy, RPA is valid when [2]

$$\frac{\chi^2}{1+T_e}\ll 1, \qquad (3)$$

So that the potential energy of the gas remains much smaller than its kinetic energy. We recall in Fig. 1 the validity domain of the temperature-dependent RPA.

We now have to mention some additional inherent limitations to this work. They are related to the interaction between cluster and plasma.

First, we will neglect Barkas effect. It has been shown [5] that this effect appears when the projectile is too charged so that its field cannot be treated as a weak perturbation in plasma. The charge must remain lower than the number of electrons contained in a sphere with radius plasma screening length.

Second, we shall neglect the recoil energy [6,7] of the cluster in order to assume a straight-line trajectory. So its kinetic energy must remain greater than the average kinetic energy of the electrons in plasma. Assuming a cluster with velocity V and mass M, this reads as

$$\tfrac{1}{2}MV^2\gg\tfrac{1}{2}m_e V_{\rm th}^2\ .$$

So, the velocity V must fulfill $V\gg\sqrt{m_e/M}\,V_{\rm th}$. Since the considered cluster will at least contain one proton, the ratio $\sqrt{m_e/M}$ should remain smaller than $\frac{1}{43}$. We are then allowed to investigate some low-velocity effects ($V\ll V_{\rm th}$) as long as V fulfills the above condition. In the case of a degenerate plasma, the same analysis still holds by considering the Fermi velocity instead of $V_{\rm th}$.

The present paper is structured as follows.

(1) We first evaluate the stopping power by the uni-

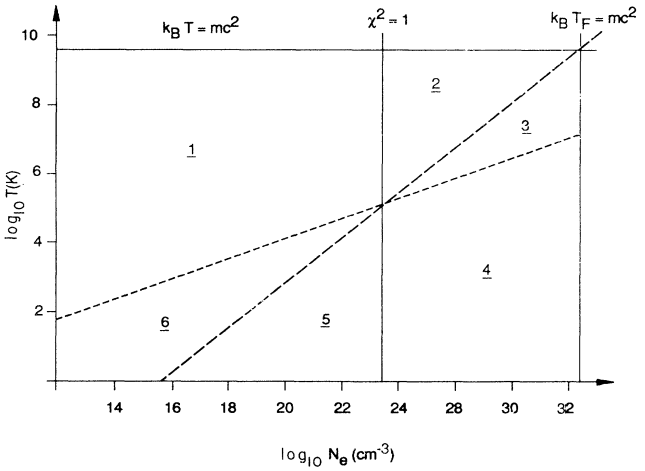

FIG. 1. Domain of validity for the temperature-dependent RPA corresponds to regions 1, 2, 3, and 4. The long-dashed line pertains to $T=T_F$ while the short-dashed line to $\Gamma_e=1$.

form free-electron gas of an extended charge within the dielectric formalism.

(2) We then briefly review the RPA dielectric formalism and make use of analytical properties for the dielectric function to exhibit at any temperature key quantities such as the critical distance of pointlike behavior for an extended charge or the critical distance of separated behavior for two charges. Asymptotic analytic expressions are worked out in the low- and high-velocity range at any temperature for an extended charge with spherical symmetry.

(3) Stopping calculations are detailed in Sec. III for a dicluster randomly oriented and in Sec. IV for an ion with an extended charge distribution.

II. STOPPING POWER OF AN EXTENDED CHARGE DISTRIBUTION

A. General formalism

For a pointlike charge Z at velocity V entering an electron gas, the energy loss by unit path length is given in the dielectric formalism by [8]

$$-\frac{dE}{dx}=\frac{Z^2}{V}\int\frac{d^3k}{(2\pi)^2}\frac{\mathbf{k}\cdot\mathbf{V}}{k^2}\mathrm{Im}\left[\frac{-1}{\epsilon(\mathbf{k},\mathbf{k}\cdot V)}\right] . \tag{4}$$

In order to study extensively the effects of the correlations upon the stopping power, we consider an extended charge $\rho(\mathbf{r})$ instead of a pointlike charge $Ze\delta(\mathbf{r})$.

Let $\rho(\mathbf{r},t)$ be a charge distribution moving at velocity $\mathbf{V}$ in the electron gas; we can write $\rho(\mathbf{r},t)$ as $\rho(\mathbf{r},t)=\int d^3u\,\rho(\mathbf{u})\delta(\mathbf{r}-\mathbf{u}-\mathbf{V}t)$, $\rho(\mathbf{u})$ being the distribution at rest.

The Fourier transform $\rho(\mathbf{k},\omega)$ is given by

$$\rho(\mathbf{k},\omega)=\int d^3u\,\rho(\mathbf{u})e^{i\mathbf{k}\cdot\mathbf{u}}\delta(\omega-\mathbf{k}\mathbf{V}) .$$

Assuming $\rho(\mathbf{r},t)$ is a small perturbation for the medium, the Fourier transform of the induced field in the medium is

$$\mathbf{E}(\mathbf{k},\omega)=-4\pi i\frac{\mathbf{k}}{k^2}\frac{\rho(\mathbf{k},\omega)}{\epsilon(\mathbf{k},\omega)} .$$

Then the induced field $\mathbf{E}(\mathbf{r},t)$ is

$$\mathbf{E}(\mathbf{r},t)=\frac{-1}{(2\pi)^2}\int d^3u\rho(\mathbf{u})\int d^3k\frac{2i\mathbf{k}}{k^2}\frac{\exp[i\mathbf{k}\cdot(\mathbf{r}-\mathbf{u}-\mathbf{V}t)]}{\epsilon(\mathbf{k},\mathbf{k}\cdot\mathbf{V})} . \tag{5}$$

The force $d\mathbf{F}$ acting on the charge $\rho(\mathbf{x})d^3x$ located at $\mathbf{x}+\mathbf{V}t$ is

$$d\mathbf{F}=\rho(\mathbf{x})\mathbf{E}(\mathbf{x}+\mathbf{V}t,t)d^3x ,$$

and the energy loss of the total distribution is obtained by summing the quantities $d\mathbf{F}\cdot\mathbf{V}$. Taking into account properties of the dielectric function we get

$$-\frac{dE}{dx}=\frac{1}{V}\int\frac{d^3k}{(2\pi)^2}\frac{\mathbf{k}\cdot\mathbf{V}}{k^2}\mathrm{Im}\left[\frac{-1}{\epsilon(\mathbf{k},\omega)}\right]|\rho(\mathbf{k})|^2 , \tag{6}$$

where $\rho(\mathbf{k})$ is the Fourier transform of $\rho(\mathbf{r})$ and $\omega=\mathbf{k}\cdot\mathbf{V}$.

One recovers the stopping power of a pointlike charge by setting $\rho(\mathbf{r})=Ze\delta(\mathbf{r})$.

In the particular case where $\rho(\mathbf{r})$ is spherically symmetric, we can integrate (6) over the azimuthal angle, so we get

$$-\frac{dE}{dx}=\Omega\int_0^{V/V_F}u\,du\int_0^{\infty}z\,dz\,\mathrm{Im}\left[\frac{1}{\epsilon(z,u)}\right]|\rho(2q_Fz)|^2 \tag{7}$$

with

$$\Omega=\frac{e^2N_e}{4\pi\epsilon_0^2m_eV^2} ,$$

where the usual dimensionless variables $z=k/2q_F$ and $u=\omega/kV_F$ have been introduced. We use the dielectric function $\epsilon(\mathbf{k},\omega)$ evaluated in the RPA at any degeneracy [9,10].

B. $\epsilon(\mathbf{k},\omega)$ behavior

The dielectric function is introduced within the framework of linear-response theory as

$$\epsilon(\mathbf{k},\omega)=1-V(k)\chi^0(\mathbf{k},\omega) \tag{8}$$

with $V(k)=e^2/(\epsilon_0k^2)$, Fourier transform of the Coulomb potential, and $\chi^0(\mathbf{k},\omega)$ linear response of a free-electron gas,

$$\chi^0(\mathbf{k},\omega)=-2\int\frac{d^3q}{[2\pi]^3}\frac{n^0(\mathbf{q}+\mathbf{k})-n^0(\mathbf{q})}{(\hbar\omega+i\eta)-(\epsilon^0_{\mathbf{q}+\mathbf{k}}-\epsilon^0_{\mathbf{q}})} , \tag{9}$$

where η is a small positive quantity, $\epsilon_q^0=\hbar^2q^2/2m_e$, and $n^0(\mathbf{q})$ is the Fermi-Dirac distribution. Using dimensionless variables z, u previously introduced, we write

$$\chi^0(\mathbf{k},\omega)=-\frac{\chi^2}{\pi}G(z,u) ,$$

$$G(z,u)=f_1(z,u)+if_2(z,u) ,$$

$$f_2(z,u)=\frac{\pi T_e}{8z}\ln\left[\frac{1+\exp[(\gamma^e-p_-^2)/T_e]}{1+\exp[(\gamma^e-p_+^2)/T_e]}\right] , \tag{10}$$

with the additional dimensionless parameters

$$T_e=T/T_F,\quad \gamma^e=\mu/\varepsilon^0{}_F=\alpha^eT_e,\quad p\pm=u\pm z ,$$

where u is the chemical potential, $\varepsilon^0{}_F$ the Fermi energy, and α^e the degree of degeneracy. $f_1(z,u)$ is computed through the Kramers-Krönig relation

$$f_1(z,u)=\frac{1}{\pi}\mathrm{P}\int_{-\infty}^{+\infty}\frac{f_2(z,t)}{t-u}dt . \tag{11}$$

f_1 and f_2 are essentially significant on a range in u (or z) measured by $A_0(T_e)$ with

$$A_0(T_e)=\frac{1}{\sqrt{2}}[\gamma^e+(\gamma^{e2}+\pi^2T_e^2)^{1/2}]^{1/2} . \tag{12}$$

Gouédard [10] showed that at any temperature, $A_0(T_e)V_F$ represents the average electron velocity; when $T_e=0$, $A_0(T_e)=1$ and when $T_e\gg1$, $A_0(T_e)V_F\approx V_{\mathrm{th}}$,

$$f_1(z,u)\leq 0 \quad \text{for } u \geq A_0(T_e) ,$$

$$f_2(z,u)\approx 0 \quad \text{as soon as } |z-u| \geq A_0(T_e) .$$

The equation $\epsilon(z_r,u_r)=0$ can be solved. One thus gets for the real part of z_r and u_r at resonance

$$z_r^2=\frac{\chi^2}{3u_r^2}\left[1+\frac{T_e F_{3/2}(\alpha^e)}{u_r^2 F_{1/2}(\alpha^3)}+\frac{T_e^2 F_{5/2}(\alpha^e)}{u_r^4 F_{1/2}(\alpha^e)}\right] , \qquad (13)$$

$$u_r \geq A_0(T_e) ,$$

where

$$F_n(x)=\int_0^\infty [t^n/(1+e^{t-x})]dt$$

is the Fermi function of nth order.

At first order, $z_r^2=\chi^2/3u_r^2$ corresponds to $\omega=\omega_p$. We study first the behavior of $\mathrm{Im}[1/\epsilon(z,u)]$ in the z-u plane. Figure 2 displays the two domains where this function takes values in the integration range of Eq. (7).

Region (a) where $|z-u|<A_0(T_e)$, which pertains to binary collisions. The corresponding energy exchange is $\hbar\omega\approx\hbar^2q^2/2m_e$.

Region (b) corresponds to the resonance with $z \ll A_0(T_e)$ and $u > A_0(T_e)$ where the projectile charge yields its energy to the collective mode with resonance at $z=z_r$ and energy exchange close to $\hbar\omega=\hbar\omega_p$. At $T=0$, the resonance curve becomes a δ function while $A_0(T_e)=1$. One then recovers the behavior of $\mathrm{Im}(1/\epsilon)$ as evaluated by Lindhard [8] at $T=0$.

We see from Fig. 2 that the main contribution to (7) arises from values of $z<Z_m=V/V_F+A_0(T_e)$ because $\mathrm{Im}[1/\epsilon(z,u)]$ is negligible for larger z. Therefore we can say that $\mathrm{Im}[1/\epsilon(\mathbf{k},\omega)]$ does not take significant values for $k>k_m=2q_FZ_m$. In the same way, we see that if $V/V_F \gg A_0(T_e)$, the main contribution to the z integral in (7) arises from z larger than $z_r(V/V_F)$.

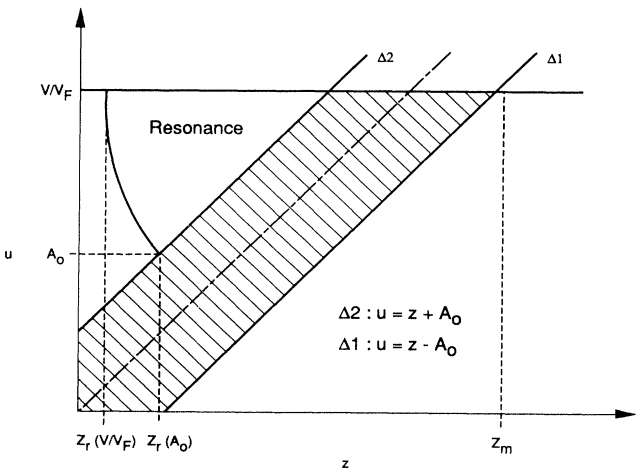

FIG. 2. Domain of importance of $\mathrm{Im}[1/\epsilon(z,u)]$ in the z-u plane. Region (a) is hatched while region (b) is around the resonance curve.

C. Stopping power

We now investigate some consequences of the analytic structure of the dielectric function upon the stopping power.

We first look for the condition to be fulfilled by a charge to act in a pointlike fashion. Suppose we have a distribution $\rho(\mathbf{r})$ which is enclosed in a sphere of radius R, then in the Fourier transform $\rho(\mathbf{k})=\int d^3\mathbf{r}\,\rho(\mathbf{r})e^{i\mathbf{k}\cdot\mathbf{r}}$, we write $\mathbf{k}\cdot\mathbf{r}<kr<kR$. If $k_mR \ll 1$ we can set $e^{i\mathbf{k}\cdot\mathbf{r}}\sim 1$ without changing result (6). Therefore we get $\rho(\mathbf{k})\approx\int d^3r\,\rho(\mathbf{r})$ equal to the total charge so that the extended charge may be taken to be pointlike. The criterion appears to be

$$R \ll 1/k_m \Longleftrightarrow R \ll 1/2q_FZ_m ,$$

i.e.,

$$R \ll \frac{1}{2q_F[V/V_F+A_0(T_e)]}=R_0 , \qquad (14)$$

which can be rewritten as

$$R_0=\frac{\lambda\!\!\!^{-}}{2[V/A_0(T_e)V_F+1]} . \qquad (15)$$

If we define $\lambda\!\!\!^{-}$, the de Broglie wavelength by

$$\lambda\!\!\!^{-}=\frac{\hbar}{m_eV_FA_0(T_e)} .$$

At any velocity and temperature, R_0 defines a critical distance of pointlike behavior.

Obviously two charges separated by a long distance will not be affected by the stopping correlations. Let $\rho(\mathbf{r})$ be written as $\rho(\mathbf{r})=\rho_1(\mathbf{r})+\rho_2(\mathbf{r}-\mathbf{R})$, the superposition of two distributions separated by $\mathbf{R}$. We have $\rho(\mathbf{k})=\rho_1(\mathbf{k})+\rho_2(\mathbf{k})\exp[i\mathbf{k}\cdot\mathbf{R}]$ and

$$|\rho(\mathbf{k})|^2=\rho(\mathbf{k})\rho(\mathbf{k})^*=|\rho_1(\mathbf{k})|^2+|\rho_2(\mathbf{k})|^2 + \{\rho_1(\mathbf{k})\rho_2(\mathbf{k})^*\exp[-i\mathbf{k}\cdot\mathbf{R}] + \rho_1(\mathbf{k})^*\rho_2(\mathbf{k})\exp[i\mathbf{k}\cdot\mathbf{R}]\} .$$

Inserting this expression in Eq. (1), we obtain a sum of three terms, the stopping powers of ρ_1 and ρ_2 and a correlation term. Suppose that ρ goes faster than $V_FA_0(T_e)$, we see that the main contribution to the integral arises from the $\mathbf{k}$ domain with $k>2q_Fz_r(V/V_F)$.

If $R \gg 1/2q_Fz_r(V/V_F)$ then the correlation quadrature almost vanishes and the stopping is the stopping power sum $\rho_1+\rho_2$; the two charges act as if they were separated. The dynamical critical distance thus exhibited,

$$R_1=\frac{1}{2q_Fz_r(V/V_F)} , \qquad (16)$$

yields V/ω_p if we restrict to lowest order in Eq. (13).

At high velocity, the screening distance of the plasma plays a particular role; it can be seen from Fig. 2 that if $2q_Fz_r(A_0)R \ll 1$ we can take the charges as coagulated as far as the plasmons excitation are concerned in view of $\exp[\pm i\mathbf{k}\cdot\mathbf{R}]\approx 1$ all along the resonance curve. The dis-

tance $R_2=1/[2q_F z_r(A_0)]$ coincides with the static Thomas-Fermi length or the Debye length whether the plasma is degenerate or not. The screening distance of the plasma then corresponds to charges coagulation with respect to plasmon excitation.

For the low-velocities case we consider pointlike charges to investigate how varying separating distance affects stopping power. When two ions enter the target plasma they induce a field $\mathbf{E}_{\text{ind}}$ in it which stops them. The field acting upon an ion is the superposition of the field $\mathbf{E}_0$ it creates in the plasma and the field $\mathbf{E}_1$ created by the other ion. When the interion distance increases, the correlation part of the stopping power vanishes because $\mathbf{E}_1$ gets screened by the plasma. Since in the low-velocity case we expect the perturbation created by the cluster to be static, the distance of separation is the screening distance of the plasma. The behavior of this quantity has been studied in the RPA at any degeneracy [9,10]. The screening distance relies on the plasma parameters as follows:

(i) Classical plasma, $T > T_F$ where the screening distance is λ_{Debye}.

(ii) Weakly degenerate plasma, $T_F > T > 0.106 r_s$, where the screening distance is λ_{TF}.

(iii) Strongly degenerate plasma acting like a Fermi liquid with Friedel screening $\cos(2q_F r)/(2q_F r)^3$.

We show in Fig. 3 the shape of those three domains in the N-T plane and sum up the previous results in Table I.

Expression (6) shows that the stopping power depends on the shape of the distribution through the square modulus of its Fourier transform. Then all the charges having a Fourier transform with the same modulus will be stopped a same amount in a given target. Let ρ^0 be a test charge; in Fourier space a charge equivalent to ρ^0 can be written as $\rho(\mathbf{k})=|\rho^0(\mathbf{k})|e^{i\phi(\mathbf{k})}$. Because $\rho(\mathbf{r})$ must be a real function, $\phi(\mathbf{k})$ is an odd function of $\mathbf{k}$. Then in the real space the shape of $\rho(\mathbf{r})$ must be

$$\rho(\mathbf{r})=\rho^0(\mathbf{r})\otimes\mathcal{F}^{-1}\{e^{i\phi(\mathbf{k})}\} ,$$

$$\phi(\mathbf{k}) \text{ odd} ,$$

where $\otimes$ denotes a convolution product and $\mathcal{F}^{-1}$ the inverse Fourier transform.

We finally consider an extended charge with spatial extension ΔR. It is well known that in Fourier space, the "size" of the distribution will be approximately Δk linked to ΔR by the relation

$$\Delta R\,\Delta k \approx 1 \quad \text{so that} \quad \Delta k \approx \Delta R^{-1} .$$

The study of $\text{Im}(1/\epsilon)$ showed that in the high-velocity range this function does not take significant values for $k < k_{\min}=2q_F z_r(V/V_F)$. If $\Delta R \gg 1/k_{\min}=R_1$ then the charge will appear quasitransparent for the plasma, interacting only with a few long-range binary collisions without losing energy through plasmon excitation.

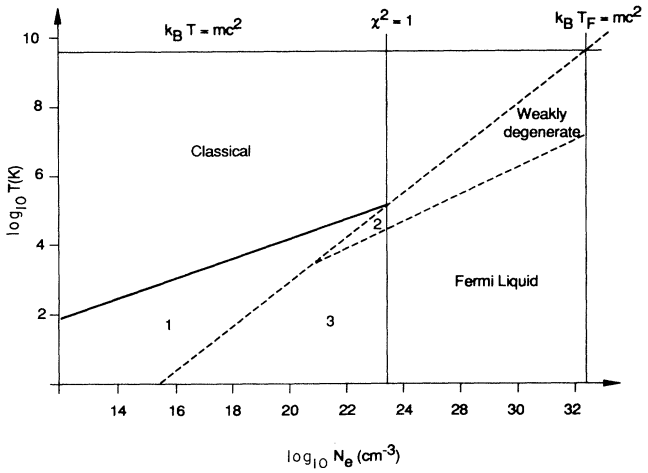

FIG. 3. Regions of different kind of screening. The long-dashed line indicates the $T=T_F$ limit while the short-dashed line shows the frontier $T_e=0.106 r_s$. The screening is Debye in the classical area, Thomas-Fermi in the weakly degenerate domain, and Friedel in the Fermi liquid. Domains 1, 2, and 3 correspond to strongly coupled plasmas.

TABLE I. Critical distances of pointlike and separate behavior in terms of the velocity. R_0, R_1 given by Eqs. (15) and (16).

	Pointlike	Separate
High velocity, $V > V_F A_0$	R_0	R_1
Low velocity, $V < V_F A_0$	R_0	λ_{screen}

D. Asymptotic stopping power

We now investigate some asymptotic expressions of $(dE/dx)/\Omega$ [where dE/dx is given by Eq. (7)] in the high- and low-velocity range, respectively.

In the high-velocity range, i.e., velocity larger than the average electron velocity in gas, we use a method proposed by Lindhard for a pointlike ion. Instead of integrating z from zero to infinity and u from zero to V/V_F, Lindhard proposed to integrate z from $z_r(V/V_F)$ to V/V_F and u from zero to infinity. We show schematically in Fig. 4 the resulting discrepancy. Maynard and

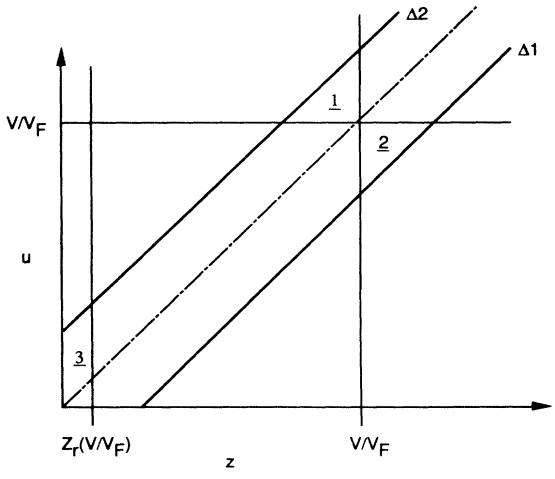

FIG. 4. Switching the integration domain of Eq. (7) according to Lindhard method, we drop the quadrature on regions 2 and 3 while we add the one on 1. The corresponding unaccuracy decreases as $1/V^4$.

Deutsch [3] proved that for any temperature it decays as $1/V^4$, thus the expansion obtained by integrating on the modified domain is exact up to the third order in $1/V$. In fact, there is no third-order term in the case of a pointlike ion, so this method provides the exact second-order term. In this case, the u quadrature is evaluated by the sum rule

$$\int_0^\infty \omega \,\mathrm{Im}\left[\frac{1}{\epsilon(q,\omega)}\right] d\omega = \frac{\pi\omega_p^2}{2} .$$

Finally, a good approximation for the stopping power of a pointlike charge Z in the high-velocity range is given by

$$\frac{1}{\Omega}\frac{dE}{dx} = Z^2 \int_{z_r(V/V_F)}^{V/V_F} \frac{dz}{z} . \tag{17}$$

It is easily shown that the same approximation still holds for an extended charge. We thus get

$$\frac{1}{\Omega}\frac{dE}{dx} = \int_{z_r(V/V_F)}^{V/V_F} \frac{|\rho(2q_F z)|^2}{z} dz . \tag{18}$$

In the low-velocity range, following Maynard and Deutsch [1], one can derive

$$\frac{dE}{dx} = \frac{e^2}{2\pi^2\epsilon_0^2 V_F^2} N_e \left[\frac{V}{A_0(T_e)V_F}\right] \Phi ,$$

where

$$\Phi = \frac{\pi A_0(T_e)}{2} \int_0^\infty \frac{dz\, z^3}{[z^2+\chi^2 f_1(0,0)]^2} \times \frac{|\rho(2q_F z)|^2}{1+\exp[(z^2-\gamma^e)/T_e]} . \tag{19}$$

It can be seen that the stopping power is still proportional to the velocity according to friction.

Here, $\chi^2 f_1(0,0)$ represents the static screening avoiding the well-known logarithmic divergence of classical theory, so that

$$z^2+\chi^2 f_1(0,0) = \begin{cases} \frac{1}{4q_F^2}[q^2+\lambda_{\mathrm{TF}}^{-2}], & T_e \to 0 \\ \frac{1}{4q_F^2}[q^2+\lambda_D^{-2}], & T_e \to \infty . \end{cases}$$

III. DI-CLUSTER RANDOMLY ORIENTATED

Arista [15] considered at $T=0$ a distribution such as $\rho(\mathbf{r}) = Z_1 e\delta(\mathbf{r}) + Z_2 e\delta(\mathbf{r}-\mathbf{R})$, which amounts to

$$|\rho(\mathbf{k})|^2 = (Z_1 e)^2 + (Z_2 e)^2 + 2e^2 Z_1 Z_2 \cos(\mathbf{k}\cdot\mathbf{R}) .$$

Performing an angular average upon $\mathbf{R}$ yields

$$|\rho(\mathbf{k})|^2 = (Z_1 e)^2 + (Z_2 e)^2 + 2e^2 Z_1 Z_2 \,\mathrm{sinc}(kR) , \tag{20}$$

where $\mathrm{sinc}(x) = \sin(x)/x$.

The stopping power of the dicluster can be written as

$$\left[\frac{dE}{dx}\right] = \left[\frac{dE}{dx}\right]_{Z_1} + \left[\frac{dE}{dx}\right]_{Z_2} + \left[\frac{dE}{dx}\right]_{\mathrm{corr}}$$

with

$$-\left[\frac{dE}{dx}\right]_{\mathrm{corr}} = 2Z_1 Z_2 \Omega \int_0^{V/V_F} u\, du \int_0^\infty z\, dz\, \mathrm{Im}\left[\frac{1}{\epsilon(z,u)}\right] \times \mathrm{sinc}(2q_F R z) . \tag{21}$$

A. High velocity

Using formula (18) we obtain in the high-velocity range

$$\frac{1}{\Omega}\left[\frac{dE}{dx}\right]_{\mathrm{corr}} = 2Z_1 Z_2 \int_{R_1^{-1}}^{R_0^{-1}} \frac{\sin(Rk)}{Rk}\frac{dk}{k} = H(R/R_0) - H(R/R_1) \equiv 2Z_1 Z_2 L^{\mathrm{corr}}(V) , \tag{22}$$

where $H(x) = \mathrm{Ci}(x) - \mathrm{sinc}(x)$ and $\mathrm{Ci}(x)$ is the cos integral.

Equation (22) is formally identical to its $T=0$ limit already obtained previously by Arista [3]. Temperature and degeneracy dependence only appear in the lower bound R_1^{-1}.

It is instructive to notice the behavior of Eq. (22) for large R values. For large x value, $H(x) \approx \cos(x)/x^2$ and neglecting $H(R/R_0)$, we thus get

$$\frac{1}{\Omega}\left[\frac{dE}{dx}\right]_{\mathrm{corr}} = -2Z_1 Z_2 \frac{\cos(R/R_1)}{(R/R_1)^2} , \tag{23}$$

displaying long-range oscillation of wavelength $2\pi R_1 \approx 2\pi V/\omega_p$ connected to oscillations of the screened electric field.

We plot in Figs. 5(a) and 5(b) the ratio $L^{\mathrm{corr}}(V)/L(V)$ for several degeneracies and a cluster velocity equal to three times the average electron velocity in plasma. It can thus be seen from these plots and also from the previous critical distances analysis that for high velocities the correlation effects are only weakly temperature dependent. Equations (14) and (16) yield back the high-velocity limit $R_0 \approx \hbar/2mV$ and $R_1 \approx V/\omega_p$ which are temperature independent. In fact, the correlation term of the stopping power behaves in these limits like the pointlike one. $L(V)$ is given its high V approximation expression [1]

$$L(V) = \ln\left[\frac{2mV^2}{\hbar\omega_p}\right] - T_e \frac{F_{3/2}(\alpha^e)}{F_{1/2}(\alpha^e)}\left[\frac{V_F}{V}\right]^2 - T_e^2\left[\frac{F_{5/2}(\alpha^e)}{F_{1/2}(\alpha^e)} - \frac{1}{2}\left[\frac{F_{3/2}(\alpha^e)}{F_{1/2}(\alpha^e)}\right]^2\right]\left[\frac{V_F}{V}\right]^4$$

in terms of the Fermi function introduced below Eq. (13).

B. Low velocity

The correlation part of the stopping power is given by Eq. (19) with

$$\Phi^{\rm corr}=\frac{\pi A_0(T_e)}{2}\int_0^\infty \frac{z^3dz}{[z^2+\chi^2 f_1(0,0)]^2} \times\frac{\mathrm{sinc}(2q_F Rz)}{[1+\exp(|z^2-\gamma^e|/T_e)]} . \quad (24)$$

It is easy to derive many asymptotic expressions out of Eq. (24) for low and high temperature and also small and large R. Some useful results are also obtained for large R. At high temperature, we get

$$\Phi^{\rm corr}=\pi A_0(T_e)\exp(\alpha^e)\frac{1}{(R/\lambda_D)^4}+O\left[\frac{1}{R^5}\right] . \quad (25)$$

At low temperature

$$\Phi^{\rm corr}=-\frac{2}{\pi}\frac{\cos(2q_F R)}{(2q_F R)^2}+O\left[\frac{1}{R^3}\right] . \quad (26)$$

Equations (25) and (26) show, respectively, the connection between the correlation effect and the screened field of a static point charge. At high temperature, correlation becomes negligible for R greater than Debye length. At low temperature, the Fermi-liquid behavior of electron gas arises and produces spatial oscillations of wavelength π/q_F.

The ratio of low velocity and correlated stopping to pointlike is shown on Figs. 5(c) and 5(d) at two densities and different temperature and one can witness qualitative and quantitative effects of the temperature in this case.

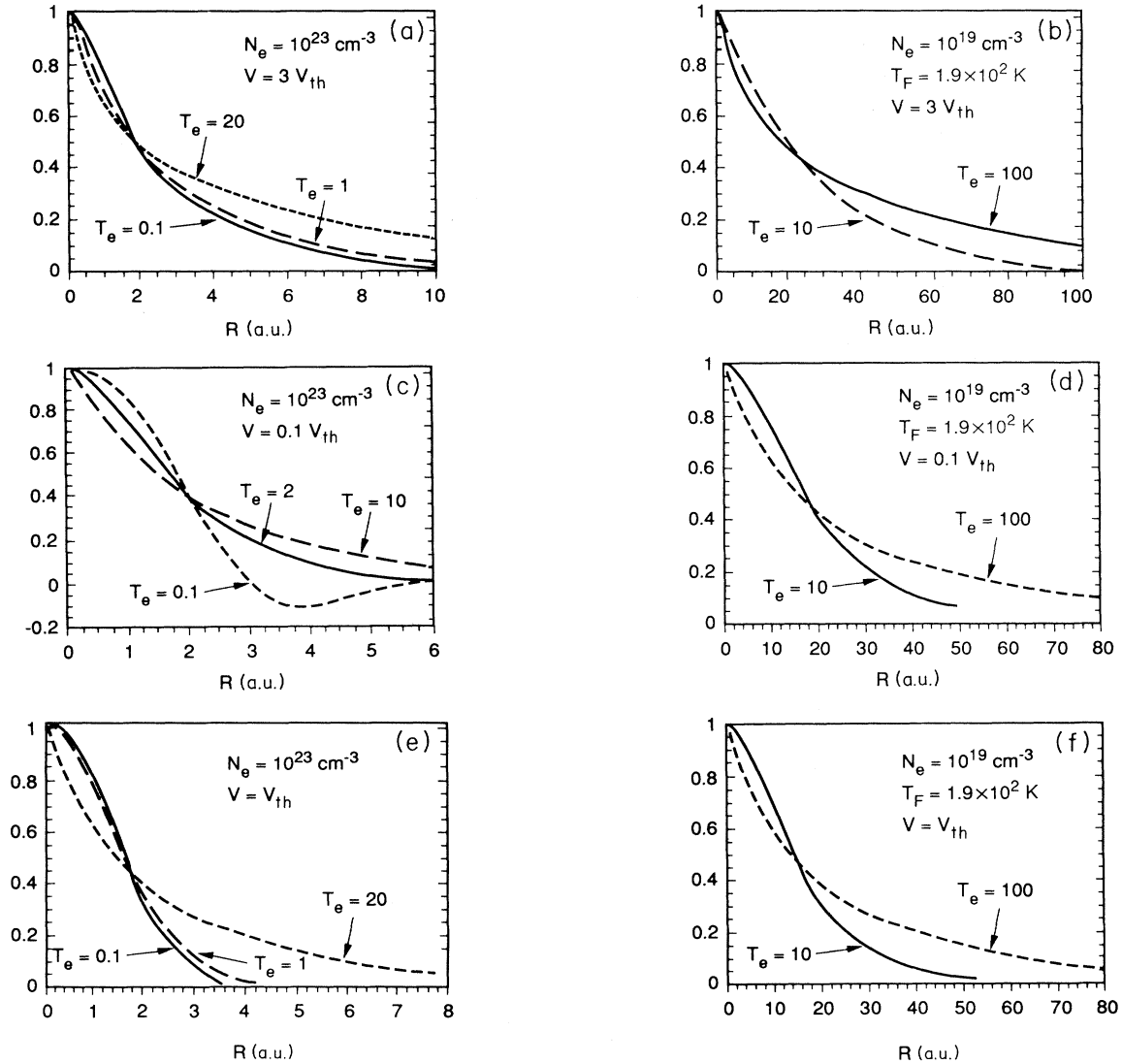

FIG. 5. Plot of the ratio (of the correlation part of stopping power) to the pointlike part of the stopping power $L^{\rm corr}(V)/L(V)$. (a) $V=3V_{\rm th}$ (or V_F), $N_e=10^{23}$ cm^{-3}, $T_e=0.1,1,20$. (b) $V=3V_{\rm th}$, $N_e=10^{19}$ cm^{-3}, $T_e=10,100$. (c) $V=0.1V_{\rm th}$ (or V_F), $N_e=10^{23}$ cm^{-3}, $T_e=0.1,1,20$. (d) $V=0.1V_{\rm th}$, $N_e=10^{19}$ cm^{-3}, $T_e=10,100$. (e) $V=V_{\rm th}$ (or V_F), $N_e=10^{23}$ cm^{-3}, $T_e=0.1,1,20$. (f) $V=V_{\rm th}$, $N_e=10^{19}$ cm^{-3}, $T_e=10,100$. The temperature $T_e=0.1$ has been removed from the plots (b), (d), and (f) because the corresponding plasma would lie beyond the RPA domain.

Qualitatively, the transition from Friedel-like screening to Debye-like, while the temperature is increasing, damps out the oscillations observed at $T_e=T/T_F=0.1$. Quantitatively, Eq. (14) yields the low-velocity regime $R_0\approx\lambda\!\!\!^{-}/2$ [$\lambda\!\!\!^{-}$ being the de Broglie wavelength defined in Eq. (15)]. We then observe two effects when the temperature increases; R_0 decreases so the correlation effects at small distances are damped out, but as the screening length increases with temperature, the long-range effects get inflated.

The plots in Figs. 5(e) and 5(f) illustrate the situation where the cluster velocity is equal to $V_{\rm th}$ (or V_F in the degenerated case).

IV. SINGLE ION WITH EXTENDED CHARGE DISTRIBUTION

A. Ion domain of nonpunctuality

We have already seen that a charge distribution cannot be considered as pointlike if its size is larger than R_0 as defined by Eq. (15). There are many cases where that distance is shorter than atomic unit. For example, at low velocity and low temperature, R_0 reduces to $1/q_F$ while the condition for validity of RPA [1,3] requires that at low temperature $a_0\gg 1/q_F$ where a_0 is the Bohr radius. It means that in these conditions, even a single ion cannot be considered as pointlike.

Let ηa_0 be the size of an ion; in the high-velocity range, $V\gg A_0(T_e)V_F$, R_0 reduces to $V_F/(2q_FV)$ and it can be taken as pointlike if ηa_0 satisfies the inequality

$$V\ll\frac{V_F}{2q_F\eta a_0}$$

i.e., $\eta V\ll 0.5$ a.u.

Nevertheless, this condition cannot be satisfied if $A_0(T_e)V_F$ is already larger than $V_F/(2q_F\eta a_0)$, which yields

$$A_0(T_e)\gg\frac{1}{2q_F\eta a_0}\ . \tag{27}$$

In the low-velocity range, R_0 becomes $1/[2q_FA_0(T_e)]$ and the condition $\eta a_0\gg R_0$ still leads to Eq. (27). Finally, whatever its velocity, an ion of size ηa_0 cannot be considered as pointlike when Eq. (27) is satisfied.

The study of the domain defined by (27) is different whether the plasma is degenerate or not. In a classical plasma, writing $A_0(T_e)V_F=V_{\rm th}$, Eq. (27) becomes a condition on temperature, i.e.,

$$k_BT\gg(4\times10^4/\eta^2)K=(3.44/\eta^2)\ \text{eV}\ . \tag{28}$$

In a degenerate plasma, assuming $A_0(T_e)=1$ we thus get a condition on density

$$N_e\gg(2.8/\eta^3)\times10^{23}\ \text{cm}^{-3}\ . \tag{29}$$

Generally, η is a function of the charge and ionization of an ion. Of course, an extensive study of this effect should also take into account the ion ionization state. For example, if the plasma is too hot the ion will turn pointlike as it gets fully ionized.

B. Stopping power of an ion with extended charge distribution

We now consider the impact of an atom extended charge distribution upon free-electron gas stopping power. Such a survey has already been achieved by Deutsch and Maynard [11] as far as bound electrons to the target are concerned.

We thus have to consider a distribution such as

$$\rho(\mathbf{r})=Ze\delta(\mathbf{r})-n(\mathbf{r})e\ , \tag{30}$$

where $\int d^3r\,n(\mathbf{r})=N$.

Z is the number of protons in the nucleus and N the number of electrons. According to Eqs. (28)–(29) the nucleus can be considered as pointlike in all RPA plasma (setting $\eta\approx10^{-5}$, it appears that the plasma should be taken relativistic). We assume that the electronic cloud is not perturbed by the plasma, thus $n(r)$ is spherically symmetric and

$$\rho(k)=Ze-4\pi e\int dr\,n(r)r^2\text{sinc}(kr)\ .$$

We recognize here the expression of the elastic form factor already investigated [12] through the Green-Sellin-Zachor model for $n(r)$.

Setting $F(k)=4\pi\int dr\,n(r)r^2\text{sinc}(kr)$, we have (atomic units)

$$F(k)=N\eta\xi\left[\frac{A}{k^2+\xi^2(1+\alpha)^2}+\frac{B}{k^2+\xi^2(1+\beta)^2}+\frac{C}{k^2+\xi^2}\right] \tag{31}$$

with

$$DA=\left[\frac{1}{H}-\frac{1}{H^2}-\frac{2H-1-1/H^2}{(1+\beta)^2}\right],$$

$$DB=\left[\frac{1}{H^2}-\frac{1}{H}+\frac{2H-1-1/H^2}{(1+\alpha)^2}\right],$$

$$C=1/H^2,\quad D=1/(1+\alpha)^2-1/(1+\beta)^2\ ,\quad H=\eta/\xi\ .$$

The values of ξ, H, α, and β are given in Refs. [13,14]. Species considered here include Al^{3+}, Al^{8+}, Al^{11+}, and Cs^+, with corresponding parameters given in Table II.

From $F(0)=N$, one gets $F(k)=(Z-N)e+e[F(0)-F(k)]$. The last term represents a correction to the pointlike case. The square modulus of the distribution is then

TABLE II. Values of Z,N,H,ξ,α, and β for considered species. From Refs. [6,7].

Species	Z	N	H	ξ	α	β
Al^{3+}	13	10	1.211 28	3.146 5	2.450 4	1.00 9
Al^{8+}	13	5	1.194 96	4.970 2	2.354 55	1.008 8
Al^{11+}	13	2	0.845 845	16.920 6	1.629 026 4	1.018 4
Cs^+	55	54	4.531 5	1.154 7	9.302 1	1.721 85

$$|\rho(k)|^2=[(Z-N)e]^2+\{e[N-F(k)]\}^2 +2(Z-N)e^2[N-F(k)] . \quad (32)$$

The function F is decreasing, $N-F(k)>0$, and we will obtain an enhanced stopping power. Deutsch and Maynard already observed the same effect. It is worth noticing that the model can account for the stopping power of a neutral atom with $N=Z$.

The stopping power then appears as the sum of the pointlike atomic one and a correction term. In the high-velocity range, Eq. (18) yields

$$-\frac{1}{e^2\Omega}\frac{dE}{dx}=(Z-N)^2L^0(V)+N^2\int_{k_1}^{k_0}\frac{[1-F^0(a_0k)]^2}{k}dk +2N(Z-N)\int_{k_1}^{k_0}\frac{[1-F^0(a_0k)]}{k}dk , \quad (33)$$

where

$$F^0(k)=F(k)/N ,$$

$$k_1=1/R_1 ,$$

$$k_0=1/R_0, \quad L^0(V)=\int_{k_1}^{k_0}\frac{dk}{k} .$$

We investigate qualitatively a few conspicuous effects. As k_0 increases with velocity V, the correction should increase too. When temperature increases, the correction is decaying because k_1 also increases with temperature.

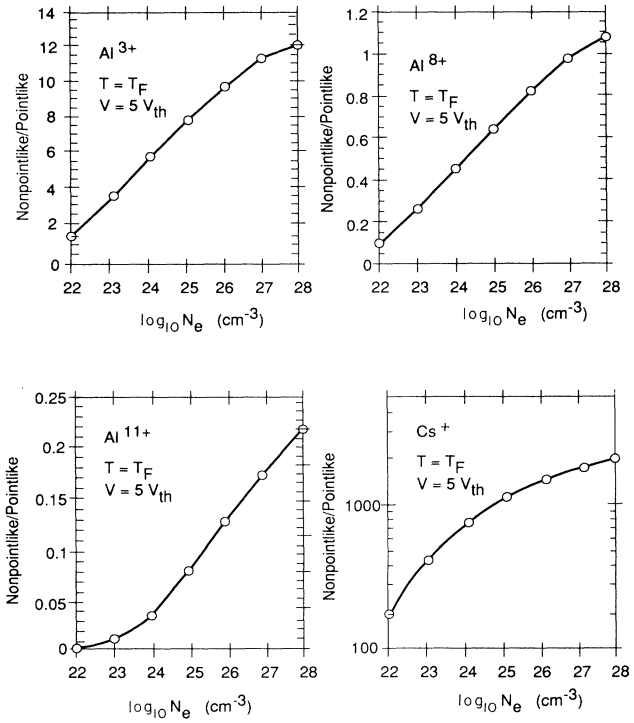

FIG. 6. Ratio of the nonpointlike stopping power to the pointlike part of the stopping power R [Eq. (34)] for the four species considered with $T=T_F$ at high velocity.

TABLE III. Values of R as given by Eq. (34) for considered species.

Species	Al^{3+}	Al^{8+}	Al^{11+}	Cs^+
R	17.7	1.64	0.4	2921

If we keep T constant, an enhanced density shall reduce T_e thus producing an enlarged correction. We define

$$R=\frac{\mathcal{C}}{(Z-N)^2L^0(V)}\approx\frac{N^2+2N(Z-N)}{(Z-N)^2}=\frac{1+2(\nu-1)}{(\nu-1)^2} , \quad (34)$$

$$\nu=Z/N ,$$

where $\mathcal{C}$ represents the correction term in Eq. (33).

We plot in Fig. 6 the numerical evaluation of R for four ions: Al^{3+}, Al^{8+}, Al^{11+}, and Cs^+; the order of magnitude of R (Table III) obtained by Eq. (34) agrees with the calculation. In fact, Eq. (34) is an overestimate to the exact value. According to Eq. (34), $R<0.1$ if $\nu>14$ and $R>1$ if $\nu<3$.

In the low-velocity range, we make use of (19) to calculate Φ under the form

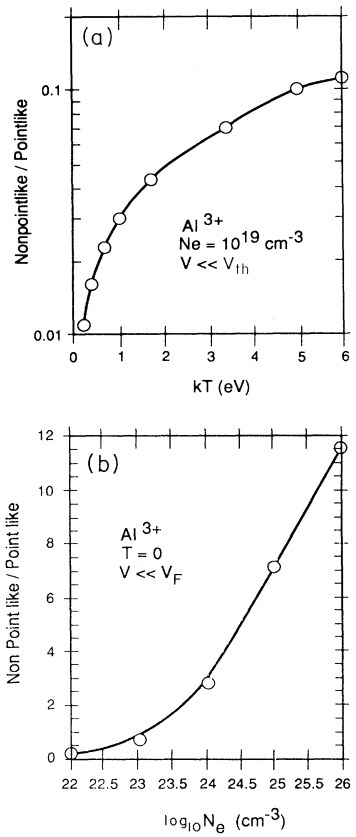

FIG. 7. Ratio of the nonpointlike stopping power to the pointlike part of the stopping power R' [Eq. (36)] for Al^{3+} at low velocity in (a) classical plasma and (b) fully degenerate plasmas.

$$\frac{2}{\pi A_0(T_e)}\Phi=(Z-N)^2\Phi^0+N^2\int_0^\infty Q(z)[1-F^0(2q_Fa_0z)]^2dz+2N(Z-N)\int_0^\infty Q(z)[1-F^0(2q_Fa_0z)]dz \tag{35}$$

with

$$Q(z)=\frac{z^3\{1+\exp[(z^2-\gamma^e)/T_e]\}^{-1}}{[z^2+\chi^2f_1(0,0)]^2},$$

$$\Phi^0=\int_0^\infty Q(z)dz .$$

The considerations made previously for the ratio R still stand for R' with

$$R'=\frac{\mathcal{C}'}{(Z-N)^2\Phi^0} \tag{36}$$

where $\mathcal{C}'$ represents correction terms. We plot on Fig. 7 the behavior of R' at high and low temperature for Al^{3+}.

V. CONCLUSIONS

We made use of the Born random-phase approximation [3] to investigate dicluster stopping of pointlike charges (Sec. III) and also of spherical symmetric ion charge distribution (Sec. IV) in a partially degenerate and uniform electron fluid.

The target plasmon contribution has been carefully assessed.

Dicluster stopping worked out in a randomly oriented model extends to arbitrary target temperatures, an approach previously devoted to the fully degenerate case [15–19]. In so doing, we have bridged a gap between condensed-matter-like jellium to classical plasma encountered in many thermonuclear fusion devices. Critical distances of pointlike and separated behaviors embody the temperature dependence of correlated charge stopping. This formalism has then been straightforwardly adapted to a spherically symmetric single-ion charge distribution worked out in a Thomas-Fermi-like approach. This extends previous results [11] obtained for cold targets to hot ones, where stopping is produced by bound electrons.

ACKNOWLEDGMENT

The Laboratorie de Physique des Gaz et des Plasmas is "Unité de Recherche Associée au CNRS."

[1] C. Deutsch, Ann. Phys. (Paris) **1**, 111 (1986); Laser Part. Beams **2**, 449 (1984).
[2] R. C. Arnold and Y. Meyer-ter-Vehn, Rep. Prog. Phys. **50**, 559 (1987).
[3] G. Maynard and C. Deutsch, J. Phys. (Paris) **46**, 1113 (1985); Phys. Rev. A **26**, 665 (1982).
[4] C. Deutsch, Laser Part. Beams **8**, 541 (1990); **10**, 315 (1992).
[5] T. Peter and J. Meyer-ter-Vehn, Phys. Rev. A **43**, 1998 (1991).
[6] D. Pines and P. Nozières, *The Theory of Quantum Liquids* (Benjamin, New York, 1966).
[7] D. Pines, *Elementary Excitations in Solids* (Benjamin, New York, 1964).
[8] J. K. Lindhard, K. Dan. Vidensk. Selsk. Mat. Fys. Medd. **28**, No. 8 (1954).
[9] C. Gouédard and C. Deutsch, J. Math. Phys. **19**, 32 (1978).
[10] C. Gouédard, Thèse de troisième cycle, Laboratoire de Physique des Gaz et des Plasmas, Orsay, 1977 (unpublished).
[11] C. Deutsch and G. Maynard, Phys. Rev. A **40**, 3209 (1989).
[12] A. E. S. Green and R. H. Garvey, Phys. Rev. **13**, 931 (1976).
[13] A. E. S. Green, D. L. Sellin, and A. S. Zachor, Phys. Rev. **184**, 1 (1969).
[14] A. E. S. Green, R. H. Garvey, and C. H. Jackman, Phys. Rev. **184**, 1 (1969).
[15] N. R. Arista, Phys. Rev. B **18**, 1 (1978).
[16] N. R. Arista and A. Gras-Marti, J. Phys. Condens. Matter **3**, 793 (1991).
[17] G. Basbas and R. H. Ritchie, Phys. Rev. A **25**, 1943 (1982).
[18] M. Vicanek, I. Abril, N. R. Arista, and A. Gras-Marti, Phys. Rev. A **46**, 5745 (1992).
[19] I. Abril, M. Vicanek, A. Gras-Marti, and N. R. Arista, Nucl. Instrum. Methods **B67**, 56 (1992).